Techniques for obtaining analytical solutions to the multicylinder somatic shunt cable model for passive neurones

J. D. Evans,* G. C. Kember,‡ and G. Major*
*University Laboratory of Physiology, Oxford OX1 3PT, United Kingdom; and ‡Beak Consultants, Brampton, Ontario, Canada L6T 5B7

ABSTRACT The somatic shunt cable model for neurones is extended to the case in which several equivalent cylinders, not necessarily of the same electrotonic length, emanate from the cell soma. The cable equation is assumed to hold in each cylinder and is solved with sealed end conditions and a lumped soma boundary condition at a common origin. A Green's function (G) is defined, corresponding to the voltage response to an instantaneous current pulse at an arbitrary point along one of the cylinders. An eigenfunction expansion for G is obtained where the coefficients are determined using the calculus of residues and compared with an alternative method of derivation using a modified orthogonality condition. This expansion converges quickly for large time, but, for small time, a more convenient alternative expansion is obtained by Laplace transforms. The voltage response to arbitrary currents injected at arbitrary sites in the dendritic tree (including the soma) may then be expressed as a convolution integral involving G. Illustrative examples are presented for a point charge input.

INTRODUCTION

In recent years, the passive electrical properties of nerve cells have been studied widely using the Rall cable model. Rall's model consists of an equivalent cylinder representing a dendritic tree coupled to a lumped impedance representing the soma (or cell body). The reduction of an entire dendritic tree to a single equivalent cylinder may take place when appropriate symmetry and other requirements are met, as detailed in Rall (1962). In fact, this reduction may still occur when some of the symmetry considerations are relaxed (as discussed, for example, in Walsh and Tuckwell, 1985). The representation of the soma as a lumped R-C circuit is based on soma isopotentiality, as discussed in Rall (1959, 1960). A summary of the assumptions, together with the governing equations, can be found in Jack et al. (1975) and Rall (1977).

An extension of the Rall model is the somatic shunt cable model, details of which can be found in Durand (1984), Kawato (1984), and Poznanski (1987 *a*, *b*). In summary, the model introduces a shunt at the soma of the Rall model, which allows a lower somatic time constant τ_s compared with the membrane time constant τ_m. Consequently, a somatic shunt parameter ϵ, defined as the ratio between the somatic and dendritic membrane time constants ($\epsilon = \tau_s/\tau_m$), is introduced into the Rall model. The shunt is interpreted as being due to either electrode penetration damage or a lower membrane resistance in the soma than in the dendrites. The refinement of the Rall model to include a shunt parameter increases the number of types of neurones to which the model can be fitted.

The single cylinder case for both the Rall cable model and the somatic shunt cable model has been solved in detail for a range of boundary conditions and input currents. A summary of the analytical progress made for both these models can be found in Poznanski (1987 *a*). Bluman and Tuckwell (1987) complete the analysis of the Rall model in the sense that they present efficient techniques for calculating the voltage response along a cylinder for any input currents. Bluman and Tuckwell demonstrated these methods (without loss of generality) for the particular case of a cylinder with a sealed end boundary condition. For examples of other types of boundary conditions, see Rall (1969, pp. 1501–1502). Although these techniques were presented for the Rall model, they extend immediately to the somatic shunt model (see Poznanski 1987*b*).

Generalization from single-cylinder models to multicylinder models has been considered but not in as much detail (see, for example, Segev and Rall, 1983; Holmes and Rall, 1987). Tuckwell (1987) outlines an indirect way of solving the multicylinder problem for the special case when each cylinder has the same length. However, the method involves solving only a single cable equation with specified boundary and initial conditions at each stage and relies on the reduction of several cylinders to one equivalent cylinder. This reduction is only possible when each cylinder is of the same electrotonic length, but in general this is not the case, and we are left with the multicylinder case (which has not yet been considered). Rall (1969) considers several equivalent cylinders of different electrotonic length for his model neurone, obtaining a transcendental equation for the equalizing time constants, but does not solve for the voltage distribution.

In this paper we generalize the single cylinder case considered by Durand (1984), Kawato (1984), and Poznanski (1987*a*, *b*) to the multicylinder case (see Fig. 1*A*). The geometry of the multicylinder case introduces several mathematical problems characterized by equations with discontinuous coefficients, which do not arise in the single cylinder case. We obtain the small time

Address correspondence to Dr. Evans.

0006-3495/92/08/350/16 $2.00

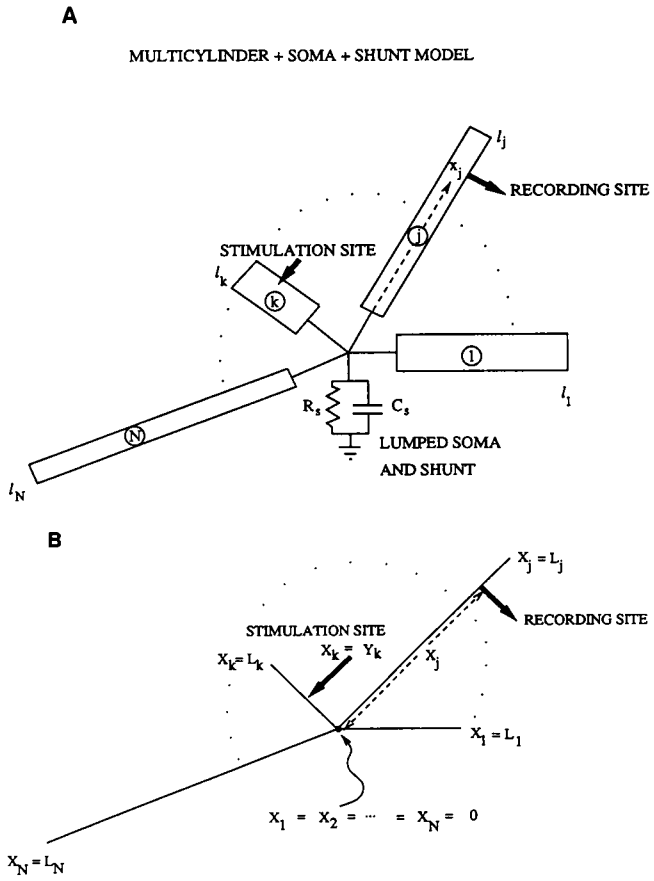

FIGURE 1 (*A*) The multicylinder somatic shunt cable model with N equivalent cylinders emanating from a common soma. (*B*) Illustration of the domain for the mathematical model representing Fig. 1 *A*.

behavior of the voltage response using Laplace transforms and series expansions and the large time behavior using an eigenfunction expansion. The large time expansion coefficients, which satisfy the initial condition, are found using two methods: the first method uses the Laplace transform result and complex residues and the second method uses a series of nonorthogonal functions and a modified orthogonality condition, similar to that proved in Churchill (1942). Because this paper, in the most part, parallels the treatment by Bluman and Tuckwell (1987) of the single cylinder Rall model, reference is made to the mathematical details derived by Bluman and Tuckwell (1987) wherever possible. Finally, we would like to note that due to a direct analogy between the heat equation and the cable equation (see Rall, 1977), the techniques used in this paper to analyze the cable equation are the same as those used in heat transfer (see, for example, Carslaw and Jaeger, 1959).

LIST OF SYMBOLS

A_{kn}	expansion coefficients, (Eq. 4.30)
B_{jn}	expansion coefficients, (Eq. 4.34)
c_{mj}	membrane capacitance per unit length of the jth cylinder [F/cm]
C_m	specific membrane capacitance [F/cm^2]
$C_s = \pi d_s^2 C_m$	lumped capacitance of soma [F]
d_j	diameter of jth cylinder [cm]
d_s	soma diameter [cm]
f_j	initial voltage distribution in jth cylinder [V]
F_j	dimensionless initial voltage distribution in jth cylinder, (Eq. 3.6)
$F(X)$	function of the initial voltage distribution defined for the whole cell, jth component is $F_j(X_j)$ when $X = X_j$
$F_s = F(0)$	value of F at the soma
$g_s = g_{sh} + g_{sm}$	soma conductance, including shunt [Ω^{-1}]
$g_{sh} = 1/R_{sh}$	somatic shunt conductance [Ω^{-1}]
$g_{sm} = \pi d_s^2/R_m$	soma membrane conductance [Ω^{-1}]
$g_{\infty j} = 1/\sqrt{r_{mj} r_{aj}}$	input conductance of the jth cylinder's infinite extension [Ω^{-1}]
$G_j^k(Y_j, Y_k, T)$	Green's function at X_j in jth branch for unit impulse at Y_k in kth branch, (Eq. 4.1)
$G_s^k(Y_k, T)$	Green's function at soma for unit impulse at Y_k in kth branch, (Eq. 4.2)
$G_j^s(X_j, T)$	Green's function at X_j in jth branch for unit impulse at soma, (Eq. 5.4)
$G_s^s(T)$	Green's function at soma for unit impulse at soma, (Eq. 5.4)
$h = \gamma/\epsilon$	a constant
$H_j^k(X_j, Y_k, T)$	solution of the Boundary Value Problem (BVP) (Eqs. 4.20–4.23, 4.28, 4.29)
i_j	applied current density to jth cylinder [A/cm]
i_s	applied current to the soma [A]
I_j	dimensionless applied current to jth cylinder, (Eq. 3.6)
I_s	dimensionless applied current to soma, (Eq. 3.6)
$K_j(X_j, Y_k, T)$	solution of the BVP (Eqs. 4.24–4.29)
l_j	physical length of jth cylinder [cm]
$L_j = l_j/\lambda_j$	electrotonic length of jth cylinder [dimensionless]
N	number of equivalent cylinders coupled at the soma
p	Laplace transform variable
$q = \sqrt{1+p}$	
Q_0	initial input charge [C]
$r_{aj} = 4R_i/\pi d_s^2$	axial resistance per unit length of jth cylinder [Ω/cm]
$r_{mj} = R_m/\pi d_j$	membrane resistance of a unit length of the jth cylinder [Ω cm]
R_i	axial resistivity [Ω cm]
R_m	membrane specific resistance [Ω cm^2]
R_s	lumped resistance of soma [Ω], (Eq. 6.2)
R_{sh}	somatic shunt resistance [Ω]
S_{jn}	index set for the eigenvalue β_{jn}, (Eq. 4.50)
t	time [s]
$T = t/\tau_m$	dimensionless time variable
v_j	transmembrane potential of jth cylinder relative to resting potential [V]
v_s	transmembrane potential of soma relative to resting potential [V]
V_j	dimensionless transmembrane potential of jth cylinder, (Eq. 3.6)

V_s	dimensionless transmembrane potential of soma, (Eq. 3.6)
x_j	physical distance along the jth cylinder [cm]
X	position variable defined for the whole cell, $X = X_j$ for the jth segment and $X = 0$ at the soma ($X_1 = X_2 = \cdots = X_N = 0$)
$X_j = x_j/\lambda_j$	electrotonic distance for the jth cable [dimensionless]
Y_k	input site for point charge

Greek symbols

α_n	eigenvalues for the H_j^k BVP, (Eq. 4.33)
β_{jn}	eigenvalues for the K_j^k BVP, (Eq. 4.36)
$\delta(\xi)$	Dirac delta function at $\xi = 0$
$\epsilon = \tau_s/\tau_m$	somatic shunt parameter [dimensionless]
θ_n	a function of α_n, (Eq. 4.41)
$\gamma = \sum_{j=1}^{N} \gamma_j$	a constant
$\gamma_j = \rho_{\infty j}$	ratio of the input conductance of the jth cylinder's infinite extension to the somatic conductance, (Eq. 3.8)
$\lambda_j = \sqrt{r_{mj}/r_{aj}}$	space constant of the jth cylinder [cm]
Λ_j	set of eigenvalues for K_j^k, (Eq. 4.38)
σ	a function of q, (Eq. 4.11)
$\tau_m = R_m C_m$	membrane time constant [s]
$\tau_s = R_s C_s$	somatic time constant [s]
$\psi_{jn}(X_j)$	eigenfunction in jth segment with eigenvalue α_n, (Eq. 4.32)
$\Psi_n(X)$	eigenfunction defined on the whole cell, being ψ_{jn} in segment j
$\phi_{jn}(X_j)$	eigenfunction in jth segment with eigenvalue β_{jn}, (Eq. 4.35)

THE MATHEMATICAL MODEL

We consider a neurone composed of a soma and N dendritic trees. We assume that each dendritic tree may be reduced to an equivalent cylinder (see Rall, 1977) so that the nerve cell may be represented by N equivalent cylinders, not necessarily of the same physical or electrotonic length, emanating from a uniformly polarized soma (see Fig. 1 *A*). For the jth equivalent cylinder, we let $v_j(x_j, t)$ denote the transmembrane potential in volts at a distance of x_j centimeters along the cylinder from the soma ($x_j = 0$) and at time t seconds. The physical length of the jth equivalent cylinder from the soma to its terminal is denoted by l_j. Then v_j satisfies the cable equation (see Tuckwell, 1987),

$$(\lambda_j)^2 \frac{\partial^2 v_j}{\partial x_j^2} - \tau_m \frac{\partial v_j}{\partial t} - v_j = -r_{mj} i_j \quad 0 < x_j < l_j, \quad t > 0, \tag{3.1}$$

where τ_m is the membrane time constant, $i_j(x_j, t)$ is an applied current density per unit length, λ_j is the characteristic length (or space constant), and r_{mj} is the membrane resistance of a unit length of the jth cylinder.

At the soma ($x_1 = x_2 = \cdots = x_N = 0$), there is voltage continuity,

$$v_1(0, t) = v_2(0, t) = \cdots = v_N(0, t) \equiv v_s(t) \tag{3.2}$$

and current conservation,

$$v_s(t) + \tau_s \frac{dv_s}{dt} - \sum_{j=1}^{N} \frac{R_s}{r_{aj}} \frac{\partial v_j(0, t)}{\partial x_j} = R_s i_s(t), \tag{3.3}$$

where R_s is the soma resistance, i_s is the injected current at the soma, r_{aj} is the internal resistance per unit length of the jth cylinder, and τ_s is the somatic time constant.

We assume that no current passes through the ends of the cylinders at $x_j = l_j$, which is the so-called "sealed end" condition,

$$\frac{\partial v_j(l_j, t)}{\partial x_j} = 0. \tag{3.4a}$$

A more general boundary condition would be to replace Eq. 3.4a with

$$a_j v_j + b_j \frac{\partial v_j}{\partial x_j} = c_j, \tag{3.4b}$$

where a_j, b_j, and c_j are constants. This boundary condition includes the clamped end condition when $b_j = 0$. The techniques used for obtaining solutions still apply when Eq. 3.4a is replaced by Eq. 3.4b, which is not considered because of the significant increase in algebraic detail.

Finally, we assume the cell to be initially polarized at $t = 0$ so that

$$v_j(x_j, 0) = f_j(x_j), \tag{3.5}$$

where we assume that the initial polarization is continuous across the soma.

We nondimensionalize Eqs. 3.1–3.5 with

$$x_j = \lambda_j X_j, \quad t = \tau_m T,$$

$$v_j = \frac{Q_0}{\gamma_k \tau_m} R_s V_j, \quad v_s = \frac{Q_0}{\gamma_k \tau_m} R_s V_s, \tag{3.6}$$

$$i_j = \frac{Q_0}{\gamma_k \tau_m} \frac{R_s}{r_{mj}} I_j, \quad i_s = \frac{Q_0}{\gamma_k \tau_m} I_s, \quad f_j = \frac{Q_0}{\gamma_k \tau_m} R_s F_j, \tag{3.7}$$

where Q_0 is the input charge (coulombs) and introduces the nondimensional parameters,

$$\epsilon = \frac{\tau_s}{\tau_m}, \quad \gamma_j = \frac{R_s}{\lambda_j r_{aj}}, \quad L_j = \frac{l_j}{\lambda_j}, \tag{3.8}$$

for $j = 1, \ldots, N$. The kth segment (in which the charge input is injected (see Eq. 4.1) has been taken as the reference segment. The nondimensional equations are

in $0 < X_j < L_j, \quad T > 0$

$$\frac{\partial^2 V_j}{\partial X_j^2} - \frac{\partial V_j}{\partial T} - V_j = -I_j(X_j, T); \tag{3.9}$$

$$\text{at } X_j = L_j \quad \frac{\partial V_j}{\partial X_j} = 0; \tag{3.10}$$

$$\text{at } X_j = 0 \quad V_j = V_s, \tag{3.11}$$

and

$$V_s + \epsilon \frac{dV_s}{dT} - \sum_{j=1}^{N} \gamma_j \frac{\partial V_j}{\partial X_j} = I_s(T); \tag{3.12}$$

$$\text{at } T = 0, \quad 0 \le X_j \le L_j \quad V_j = F_j(X_j); \tag{3.13}$$

for $j = 1, \ldots, N$. Fig. 1 *B* illustrates the mathematically equivalent system for the multicylinder neurone model shown in Fig. 1 *A*.

A GREEN'S FUNCTION

To write the solution for the generalized problem of Eqs. 3.9–3.13, we consider the Green's function $G_j^k(X_j, Y_k, T)$ defined as the solution of Eqs. 3.9–3.13, with

$$I_k = \delta(T)\delta(X_k - Y_k), \quad I_j = 0, \quad j = 1, \ldots, N, \quad j \neq k,$$
$$I_s = 0, \quad F_j = 0, \quad j = 1, \ldots, N. \tag{4.1}$$

We introduce the notation

$$G_j^k(0, Y_k, T) = G_s^k(Y_k, T) \tag{4.2}$$

when $X_j = 0$. The index k indicates that the stimulating site lies in the kth segment, $Y_k \in (0, L_k]$, and the index j indicates that the recording site lies in the jth segment, $X_j \in [0, L_j]$, where j is defined to be s when $X_j = 0$ (the soma). The Green's function G_j^k represents the response at X_j in the jth cable to a unit impulse current at a point Y_k along the kth cable. We note that for G_j^k, the source is confined to the interval $(0, L_k]$, that is the kth cylinder, and the point X_j where we measure G_j^k is confined to the interval $[0, L_j]$.

Laplace transform

The Laplace transform of G_j^k, defined as

$$\bar{G}_j^k(X_j, Y_k, p) = \int_0^{+\infty} e^{-pT} G_j^k(X_j, Y_k, T)\, dT, \tag{4.3}$$

satisfies

$$\text{in } 0 < X_k < L_k \quad \frac{\partial^2 \bar{G}_k^k}{\partial X_k^2} - (1 + p)\bar{G}_k^k = -\delta(X_k - Y_k); \tag{4.4}$$

$$\text{in } 0 < X_j < L_j \quad \frac{\partial^2 \bar{G}_j^k}{\partial X_j^2} - (1 + p)\bar{G}_j^k = 0, \quad j \neq k; \tag{4.5}$$

$$\text{at } X_j = L_j \quad \frac{\partial \bar{G}_j^k}{\partial X_j} = 0; \tag{4.6}$$

$$\text{at } X_j = 0 \quad \bar{G}_j^k = \bar{G}_s^k, \tag{4.7}$$

and

$$(1 + \epsilon p)\bar{G}_s^k - \sum_{j=1}^{N} \gamma_j \frac{\partial \bar{G}_j^k}{\partial X_j} = 0; \tag{4.8}$$

for $j = 1, \ldots, N$.

The solution of the problem for $\bar{G}_j^k$ (see Appendix 1 for details) is found in a manner similar to that outlined in Stakgold (1979, chapter 1). We note that the $\bar{G}_j^k$ are continuous at the soma but that their derivatives are discontinuous. For the source in the kth segment, we solve the governing equation over the three intervals $0 < X_j < L_j$, $0 < X_k < Y_k$, and $Y_k < X_k < L_k$, where $j \neq k$ (see Fig. 2). The conditions at the endpoints $X_j = L_j$ and $X_k = L_k$ are satisfied along with the usual conditions across the source, and we are left with two constants to be determined by satisfying continuity (Eq. 4.7) and the total flux condition (Eq. 4.8) at the soma. We thus obtain

$$\bar{G}_j^k = \frac{\gamma_k}{(1 + \epsilon(q^2 - 1) + q\sigma)} \times \frac{\cosh q(L_k - Y_k)}{\cosh qL_k} \frac{\cosh q(L_j - X_j)}{\cosh qL_j}, \tag{4.9}$$

for $j \neq k$, and

$$\bar{G}_k^k = \frac{\gamma_k}{(1 + \epsilon(q^2 - 1) + q\sigma)} \times \frac{\cosh q(L_k - Y_k)}{\cosh qL_k} \frac{\cosh q(L_k - X_k)}{\cosh qL_k} + \frac{1}{q} \frac{\cosh q(L_k - X_k)}{\cosh qL_k} \sinh qY_k, \quad Y_k < X_k. \tag{4.10}$$

where we define

$$q = \sqrt{1 + p}, \quad \sigma = \sum_{j=1}^{N} \gamma_j \tanh qL_j. \tag{4.11}$$

An expression for $\bar{G}_k^k$ for $X_k < Y_k$ may be obtained from Eq. 4.10 by interchanging X_k and Y_k using the fact that G_k^k is symmetric in X_k and Y_k (compare Eqs. A1.2 and A1.3 in Appendix 1). We remark that Eq. 4.10 in the one-cylinder case when $\epsilon = 1$ agrees with Eq. 2.4 in Bluman and Tuckwell (1987) and when $\epsilon \neq 1$, Eq. 4 in Poznanski (1987*b*).

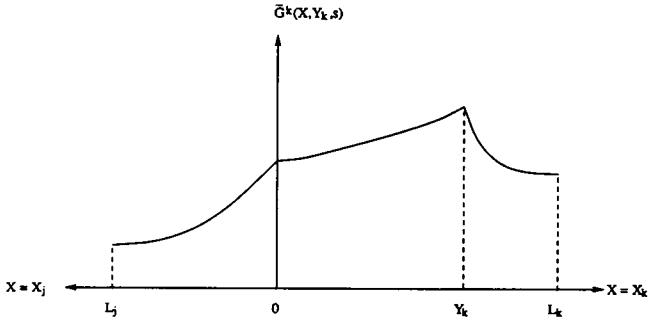

FIGURE 2 Illustration of the domain of solution for the Green's function problem $\bar{G}^k(X, Y_k, p)$, with the notation that $\bar{G}^k(X, Y_k, p) = \bar{G}_j^k(X_j, Y_k, p)$ when $X = X_j$ (i.e., the recording site is in the jth cylinder).

Small time approximation

A small time approximation is found here in the asymptotic sense: that as time is reduced, fewer terms are required to obtain a particular agreement with the exact solution. A result appropriate for small T is found by expanding Eqs. 4.9 and 4.10 for $(p, q) \gg 1$ and by using the generalized initial value theorem (Spiegel, 1965). Because the method of derivation of these expansions is presented in Bluman and Tuckwell (1987) and Poznanski (1987*b*), only the final results are presented. For $j \neq k$,

$$\bar{G}_j^k = \gamma_k \left[\frac{e^{-q(X_j+Y_k)}}{q(\gamma+\epsilon q)} + \frac{e^{-q(2L_k-Y_k+X_j)}}{q(\gamma+\epsilon q)} + \frac{e^{-q(2L_j-X_j+Y_k)}}{q(\gamma+\epsilon q)} + \frac{e^{-q(2(L_j+L_k)-X_j-Y_k)}}{q(\gamma+\epsilon q)} - \frac{e^{-q(2L_k+Y_k+X_j)}}{q(\gamma+\epsilon q)} - \frac{e^{-q(2L_j+X_j+Y_k)}}{q(\gamma+\epsilon q)} \right] + O\left(\frac{e^{-q(2(L_j+L_k)+|X_j-Y_k|)}}{q(\gamma+\epsilon q)} \right) + (1-\epsilon) O\left(\frac{e^{-q(X_j+Y_k)}}{q^2(\gamma+\epsilon q)^2} \right) + O\left(\frac{e^{-q(2(L_{\min}+X_j+Y_k)}}{q(\gamma+\epsilon q)^2} \right) \quad \text{as } q \to \infty, \tag{4.12}$$

where $L_{\min} = \min\{L_k, L_j\}$. In Eq. 4.12, we have used the order symbol O ("big oh"),[1] details of which can be found in, for example, Van Dyke (1964). Applying standard inversion formulas (see, for example, Carslaw and Jaeger, 1959, Appendix 1; Abramowitz and Stegun, 1965, p. 1020–1030), we obtain

$$\begin{aligned} G_j^k(X_j, Y_k, T) &= \gamma_k e^{-\gamma T} \left[\frac{e^{h^2T}}{\epsilon} \left\{ e^{h(X_j+Y_k)} \operatorname{erfc}\left(\frac{(X_i+Y_k)}{2\sqrt{T}} + h\sqrt{T} \right) \right. \right. \\ &+ e^{h(2L_k-Y_k+X_j)} \operatorname{erfc}\left(\frac{(2L_k-Y_k+X_j)}{2\sqrt{T}} + h\sqrt{T} \right) \\ &+ e^{h(2L_j-X_j+Y_k)} \operatorname{erfc}\left(\frac{(2L_j-X_j+Y_k)}{2\sqrt{T}} + h\sqrt{T} \right) \\ &+ e^{h(2(L_j+L_k)-X_j-Y_k)} \\ &\times \operatorname{erfc}\left(\frac{(2(L_j+L_k)-X_j-Y_k)}{2\sqrt{T}} + h\sqrt{T} \right) \\ &- e^{h(2L_k+Y_k+X_j)} \operatorname{erfc}\left(\frac{(2L_k+Y_k+X_j)}{2\sqrt{T}} + h\sqrt{T} \right) \\ &- e^{h(2L_j+X_j+Y_k)} \operatorname{erfc}\left(\frac{(2L_j+X_j+Y_k)}{2\sqrt{T}} + h\sqrt{T} \right) \\ &+ O\left(e^{h(2(L_j+L_k)+|X_j-Y_k|)} \right. \\ &\left. \left. \times \operatorname{erfc}\left(\frac{(2(L_j+L_k)+|X_j-Y_k|)}{2\sqrt{T}} + h\sqrt{T} \right) \right) \right\} \\ &+ (1-\epsilon) O(Q_1(X, Y, T)) + O(Q_2(X, Y, T)) \Big], \end{aligned} \tag{4.13}$$

where

$$\begin{aligned} Q_1 &= \frac{1}{\gamma^2} \operatorname{erfc}\left(\frac{(X_j+Y_k)}{2\sqrt{T}} \right) \\ &- \frac{2}{\epsilon\gamma} \sqrt{\frac{T}{\pi}}\, e^{-(X_j+Y_k)^2/4T} \\ &- \frac{1}{\gamma^2}(1-h-2h^2T) e^{h^2T} e^{h(X_j+Y_k)} \\ &\times \operatorname{erfc}\left(\frac{(X_j+Y_k)}{2\sqrt{T}} + h\sqrt{T} \right), \end{aligned} \tag{4.14}$$

$$\begin{aligned} Q_2 &= \frac{2}{\epsilon^2} \sqrt{\frac{T}{\pi}}\, e^{-(2L_{\min}+X_j+Y_k)^2/4T} \\ &- (2L_{\min}+X_j+Y_k+2hT) \\ &\times \operatorname{erfc}\left(\frac{(2L_{\min}+X_j+Y_k)}{2\sqrt{T}} + h\sqrt{T} \right) \end{aligned} \tag{4.15}$$

and where we define $h = \gamma/\epsilon$ with $\gamma = \sum_{j=1}^{N} \gamma_j$. Similarly, when $j = k$, we have on expanding for large q and $X_k > Y_k$, on collecting terms with the same exponential powers,

$$\begin{aligned} \bar{G}_k^k &= \frac{1}{2} \left\{ \frac{e^{-q(X_k-Y_k)}}{q} + \frac{e^{-q(2L_k-(X_k+Y_k))}}{q} \right\} \\ &+ \left(-\frac{1}{2q} + \frac{\gamma_k}{q(\gamma+\epsilon q)} \right) \left(e^{-q(X_k+Y_k)} + e^{-q(2L_k-X_k+Y_k)} \right. \\ &\left. + e^{-q(2L_k+X_k-Y_k)} + e^{-q(4L_k-X_k-Y_k)} \right) \\ &+ \left(\frac{1}{2q} - \frac{2\gamma_k}{q(\gamma+\epsilon q)} \right) e^{-q(2L_k+Y_k+X_k)} \\ &+ O\left(\left(-\frac{1}{2q} + \frac{\gamma_k}{q(\gamma+\epsilon q)} \right) e^{-q(4L_k-X_k+Y_k)} \right) \\ &+ (1-\epsilon) O\left(\frac{e^{-q(X_k+Y_k)}}{q^2(\gamma+\epsilon q)^2} \right) \\ &+ O\left(\frac{e^{-q(2L_k+X_k+Y_k)}}{q(\gamma+\epsilon q)^2} \right). \end{aligned} \tag{4.16}$$

Inverting, using standard transforms, we obtain for $X_k > Y_k$,

$$\begin{aligned} G_k^k(X_k, Y_k, T) &= \frac{1}{2} e^{-\gamma T} \left[\frac{1}{\sqrt{\pi T}} e^{-(X_k-Y_k)^2/4T} + \frac{1}{\sqrt{\pi T}} e^{-(2L_k-X_k-Y_k)^2/4T} \right. \\ &- \frac{1}{\sqrt{\pi T}} e^{-(X_k+Y_k)^2/4T} + \frac{2\gamma_k}{\epsilon} e^{h^2T} e^{h(X_k+Y_k)} \\ &\times \operatorname{erfc}\left(\frac{(X_k+Y_k)}{2\sqrt{T}} + h\sqrt{T} \right) - \frac{1}{\sqrt{\pi T}} e^{-(2L_k-X_k+Y_k)^2/4T} \\ &+ \frac{2\gamma_k}{\epsilon} e^{h^2T} e^{h(2L_k-X_k+Y_k)} \operatorname{erfc}\left(\frac{(2L_k-X_k+Y_k)}{2\sqrt{T}} + h\sqrt{T} \right) \\ &- \frac{1}{\sqrt{\pi T}} e^{-(2L_k+X_k-Y_k)^2/4T} + \frac{2\gamma_k}{\epsilon} e^{h^2T} e^{h(2L_k+X_k-Y_k)} \\ &\times \operatorname{erfc}\left(\frac{(2L_k+X_k-Y_k)}{2\sqrt{T}} + h\sqrt{T} \right) \end{aligned}$$

[1] $f(x) = O(g(x))$ as $x \to c$ if $\lim_{x \to c} [f(x)]/[g(x)] = m$, a nonzero constant.

$$
\begin{aligned}
&- \frac{1}{\sqrt{\pi T}} e^{-(4L_k - X_k - Y_k)^2/4T} + \frac{2\gamma_k}{\epsilon} e^{h^2 T} e^{h(4L_k - X_k - Y_k)} \\
&\times \operatorname{erfc}\left(\frac{(4L_k - X_k - Y_k)}{2\sqrt{T}} + h\sqrt{T}\right) \\
&+ \frac{1}{\sqrt{\pi T}} e^{-(2L_k + X_k + Y_k)^2/4T} - \frac{4\gamma_k}{\epsilon} e^{h^2 T} e^{h(2L_k + X_k + Y_k)} \\
&\times \operatorname{erfc}\left(\frac{(2L_k + X_k + Y_k)}{2\sqrt{T}} + h\sqrt{T}\right) \\
&+ O\left(\frac{1}{\sqrt{\pi T}} e^{-(4L_k - X_k + Y_k)^2/4T}\right) \\
&+ (1 - \epsilon) O(Q_3(X, Y, T)) + O(Q_4(X, Y, T))\Big], \quad (4.17)
\end{aligned}
$$

where Q_3 and Q_4 are obtained from Q_1 and Q_2, respectively, by setting $j = k$. The result for the case $X_k < Y_k$, is obtained by interchanging X_k and Y_k in Eq. 4.17, because G_k^k is symmetric in X_k and Y_k. It is useful to note that simplification of these expansions 4.13–4.17 occurs when $T \ll \epsilon^2/h^2$. Although the order of importance of the terms in the expansions 4.13 and 4.17 varies as X_k and Y_k vary, as a general guide, the terms are written in decreasing order of importance. We note that when $\epsilon \neq 1$, the term Q_1 dominates the second and successive terms included in the expansions 4.13 and 4.17, which become important only in the case $\epsilon \sim 1$.

Large time approximation

A large time approximation is found here in the asymptotic sense: that as time is increased, fewer terms are required to obtain a particular agreement with the exact solution. A large time approximation is found by using the following method that uses eigenfunction expansions to find $G_j^k(X_j, Y_k, T)$. The problem for G_j^k may be defined alternatively by Eqs. 3.9–3.13 with

$$
\begin{aligned}
&F_k = -\delta(X_k - Y_k), \quad F_j = 0, \quad j = 1, \ldots, N, \quad j \neq k, \\
&I_s = 0, \quad I_j = 0, \quad j = 1, \ldots, N. \qquad (4.18)
\end{aligned}
$$

We write G_j^k as the sum of two functions, H_j^k and K_j^k, as follows,

$$
G_j^k(X_j, Y_k, T) = H_j^k(X_j, Y_k, T) + K_j^k(X_j, Y_k, T), \quad (4.19)
$$

where H_j^k satisfies,

$$
\text{in } 0 < X_j < L_j, \quad T > 0 \qquad \frac{\partial^2 H_j^k}{\partial X_j^2} - \frac{\partial H_j^k}{\partial T} - H_j^k = 0; \quad (4.20)
$$

$$
\text{at } X_j = L_j \qquad \frac{\partial H_j^k}{\partial X_j} = 0; \quad (4.21)
$$

$$
\text{at } X_j = 0 \qquad H_j^k = H_s^k, \quad (4.22)
$$

and

$$
H_s^k + \epsilon \frac{dH_s^k}{dT} - \sum_{j=1}^{N} \gamma_j \frac{\partial H_j^k}{\partial X_j} = 0; \quad (4.23)
$$

for $j = 1, \ldots, N$, and K_j^k is taken to satisfy the following problem,

$$
\text{in } 0 < X_j < L_j, \quad T > 0 \qquad \frac{\partial^2 K_j^k}{\partial X_j^2} - \frac{\partial K_j^k}{\partial T} - K_j^k = 0; \quad (4.24)
$$

$$
\text{at } X_j = L_j \qquad \frac{\partial K_j^k}{\partial X_j} = 0; \quad (4.25)
$$

$$
\text{at } X_j = 0 \qquad K_j^k = 0, \quad (4.26)
$$

and

$$
\sum_{j=1}^{N} \gamma_j \frac{\partial K_j^k}{\partial X_j} = 0; \quad (4.27)
$$

for $j = 1, \ldots, N$. In this problem, not only is the function zero at the soma (Eq. 4.26), but there is also zero net flux (Eq. 4.27).

Initial conditions for the above two problems are,

at $T = 0$,

$$
\delta(X_k - Y_k) = H_k^k(X_k, Y_k, 0) + K_k^k(X_k, Y_k, 0), \quad (4.28)
$$

and

$$
0 = H_j^k(X_j, Y_k, 0) + K_j^k(X_j, Y_k, 0); \quad (4.29)
$$

for $j \neq k, j = 1, \ldots, N$.

By using separation of variables, we set

$$
H_j^k(X_j, Y_k, T) = \sum_{n=0}^{\infty} A_{kn}(Y_k) \psi_{jn}(X_j) e^{-(1+\alpha_n^2)T}, \quad (4.30)
$$

$$
H_s^k(Y_k, T) = H_j^k(0, Y_k, T) = \sum_{n=0}^{\infty} A_{kn}(Y_k) e^{-(1+\alpha_n^2)T}, \quad (4.31)
$$

in Eqs. 4.20–4.23. In view of the boundary condition at $X_j = L_j$ and the voltage continuity condition at $X_j = 0$, we can write the spatial eigenfunctions as

$$
\psi_{jn}(X_j) = \frac{\cos \alpha_n (L_j - X_j)}{\cos \alpha_n L_j}, \quad j = 1, \ldots, N. \quad (4.32)
$$

The conservation of current condition (Eq. 4.23), together with Eq. 4.22 defines the eigenvalues α_n, $n = 0, 1, 2, \ldots$, as the roots of the transcendental equation

$$
1 - \epsilon(1 + \alpha^2) = \alpha \sum_{j=1}^{N} \gamma_j \tan \alpha L_j. \quad (4.33)
$$

Similarly for K_j^k, we set

$$
K_j^k(X_j, Y_k, T) = \sum_{n=0}^{\infty} B_{jn}(Y_k) \phi_{jn}(X_j) e^{-(1+\beta_{jn}^2)T} \quad (4.34)
$$

in Eqs. 4.24–4.27. In view of the boundary conditions 4.25 and 4.26, the spatial eigenfunctions are

$$
\phi_{jn}(X_j) = \cos \beta_{jn}(L_j - X_j), \quad j = 1, \ldots, N, \quad (4.35)
$$

where the eigenvalues, β_{jn}, $n = 0, 1, 2, \ldots$, are

$$
\beta_{jn} = (2n + 1)\pi/2L_j. \quad (4.36)
$$

We now discuss the condition (Eq. 4.27). Substituting Eq. 4.34 into Eq. 4.27 gives

$$\sum_{j=1}^{N}\sum_{n=0}^{\infty}[(-1)^n\gamma_j B_{jn}\beta_{jn}e^{-(1+\beta_{jn}^2)T}] = 0. \quad (4.37)$$

For each $j = 1, \ldots, N$, we denote by Λ_j the set of eigenvalues of the K_j^k problem (Eqs. 4.24–4.27), namely

$$\Lambda_j = \{\beta_{jn}\}_{n=0}^{\infty}. \quad (4.38)$$

If the sets Λ_j, for $j = 1, \ldots, N$, are all disjoint, then Eq. 4.37, which holds for all T, gives

$$B_{jn} = 0 \quad \forall j \text{ and } \forall n. \quad (4.39)$$

However, the possibility of nonzero values for the B_{jn}'s exists if the eigenvalues from different sets coincide, which occurs if integers n and m can be found such that the ratio of the electrotonic lengths of any two cylinders, say the ith and the jth satisfy

$$\frac{L_i}{L_j} = \frac{(2n+1)}{(2m+1)}, \quad i \neq j, \quad m, n \in \{0, 1, 2, \cdots\}. \quad (4.40)$$

As an example, we consider $N = 2$, $L_1 = 1$, and $L_2 = 3$. Using Eqs. 4.36 and 4.38, we have

$$\Lambda_1 = \{(2n_1 + 1)\pi/2\}_{n_1=0}^{\infty}, \quad n_1 = 0, 1, 2, 3, \ldots,$$
$$\Lambda_2 = \{(2n_2 + 1)\pi/6\}_{n_2=0}^{\infty}, \quad n_2 = 0, 1, 2, 3, \ldots.$$

The sets Λ_1 and Λ_2 have common eigenvalues, namely those in Λ_1, which are the eigenvalues in Λ_2 for which $n_2 = (3n_1 + 1)$. Thus, Eq. 4.37, if it is to be satisfied for all T, gives

$$\gamma_1 B_{1n} - \gamma_2 B_{2(3n+1)} = 0 \quad \text{for } n = 0, 1, 2, \cdots$$

and

$$B_{2m} = 0 \quad \text{for } m = 0, 1, 2, \ldots, m \notin \{3n + 1\}_{n=0}^{\infty}.$$

The coefficients $A_{kn}(Y_k)$ and $B_{jn}(Y_k)$ in the above expansion may be determined by satisfying the initial conditions. Because the ψ_{kn}'s are nonorthogonal, the A_{kn}'s cannot be defined in the usual way, involving orthogonal functions. Instead, we present a method that uses the Laplace transform results and involves evaluating residues. For completeness, we mention in Appendix 2 an alternative method using a modified orthogonality condition to show how this technique generalizes from the one cylinder case (see, for example, Durand, 1984), to the multicylinder case. The A_{kn}'s can be derived in a closed form expression by this method, which coincides with that given by the Laplace transform method. However, the B_{jn}'s are left in series form, so this second method is useful only for determining the A_{kn}'s.

The calculus of residues

The coefficients $A_{kn}(Y_k)$ and $B_{jn}(Y_k)$ in the above expansions may be determined using the results of the Laplace transform of G_j^k in section 4.1 and the calculus of residues. Taking the Laplace transform of Eq. 4.19, using Eqs. 4.30 and 4.34, gives

$$\bar{G}_j^k(X_j, Y_k, p) = \sum_{n=0}^{\infty}\frac{A_{kn}(Y_k)\psi_{jn}(X_j)}{(1 + p + \alpha_n^2)} + \sum_{n=0}^{\infty}\frac{B_{jn}(Y_k)\phi_{jn}(X_j)}{(1 + p + \beta_{jn}^2)}, \quad (4.41)$$

for $j = 1, \ldots, N$.

Determination of the A_{kn}'s. Both Eqs. 4.9 and 4.10 and Eq. 4.41 have simple poles at $p = -(1 + \alpha_n^2)$, $n = 0, 1, 2, \ldots$. Evaluating the residues of $\bar{G}_j^k$ at $p = -(1 + \alpha_n^2)$ and $X_k = 0$ gives by standard methods of complex analysis (see, for example, Priestley, 1985, chapter 7),

$$A_{kn}(Y_k) = \lim_{p \to -(1+\alpha_n^2)}(p + 1 + \alpha_n^2)\bar{G}_s^k(Y_k, p)$$
$$= \frac{2\gamma_k}{\left(2\epsilon + \theta_n + \sum_{j=1}^{N}\gamma_j L_j \sec^2\alpha_n L_j\right)} \times \frac{\cos\alpha_n(L_k - Y_k)}{\cos\alpha_n L_k}, \quad (4.42)$$

where $\theta_n = [1 - \epsilon(1 + \alpha_n^2)]/[\alpha_n^2]$ (which corresponds to β_n in Durand, 1984), except when $\epsilon = 1$ and $n = 0$, then

$$A_{k0} = \frac{\gamma_k}{\left(1 + \sum_{j=1}^{N}\gamma_j L_j\right)}. \quad (4.43)$$

Further details are given in Appendix 3. We note for later reference that we may write Eqs. 4.42 and 4.43 in the form

$$A_{kn}(Y_k) = E_{kn}\psi_{kn}(Y_k) \quad (4.44)$$

where

$$E_{kn} = \frac{2\gamma_k}{\left(2\epsilon + \theta_n + \sum_{j=1}^{N}\gamma_j L_j \sec^2\alpha_n L_j\right)}, \quad (4.45)$$

and, when $\epsilon = 1$ and $n = 0$,

$$E_{k0} = A_{k0} = \frac{\gamma_k}{\left(1 + \sum_{j=1}^{N}\gamma_j L_j\right)}. \quad (4.46)$$

Determination of the B_{jn}'s. To determine the B_{jn}'s, we have to consider the following cases: (*a*) The case $\Lambda_k \cap \Lambda_j = \varnothing$.

In this case we note that $j \neq k$ (i.e., the recording segment cannot be the input segment) and Eq. 4.9 does not have poles at $p = -(1 + \beta_{jn}^2)$, which gives

$$B_{jn} = 0, \quad n = 0, 1, 2, \ldots, \quad j \neq k. \quad (4.47)$$

(*b*) The case $\Lambda_k \cap \Lambda_j \neq \varnothing$.

This case includes the possibility $j = k$ and occurs when the eigenvalues of the K_k^k and K_j^k, problems for the kth and jth branches, respectively, coincide. Evaluating residues at the simple poles $p = -(1 + \beta_{jn}^2)$ gives when $j \neq k$,

$$B_{jn}(Y) = \begin{cases} \dfrac{(-1)^{n+1}2(\gamma_k/L_k)}{L_j\left(\sum\limits_{i\in S_{jn}} (\gamma_i/L_i)\right)} \dfrac{\cos\beta_{jn}(L_k - Y_k)}{\sin(\beta_{jn}L_k)}, \\ \qquad\qquad \text{if } \beta_{jn} \in \Lambda_k; \\ 0, \quad \text{if } \beta_{jn} \notin \Lambda_k, \end{cases} \tag{4.48}$$

and when $j = k$,

$$B_{kn}(Y) = \frac{2}{L_k}\left(1 - \frac{(\gamma_k/L_k)}{\sum\limits_{i\in S_{kn}} (\gamma_i/L_i)}\right)\cos\beta_{kn}(L_k - Y_k), \tag{4.49}$$

where S_{jn}, for each $j = 1, \ldots, N$, is an index set defined by

$$m \in S_{jn} \quad \text{if } \beta_{mn} \in \Lambda_k \quad \text{where } m = 1, \ldots, N, \tag{4.50}$$

(i.e., it is a labeling set for all segments that have an eigenvalue that coincides with the nth eigenvalue of the jth segment.) We remark that Eq. 4.49 includes the particular case when $j = k$ (i.e., recording and stimulating in the same segment k), but $\Lambda_i \cap \Lambda_k = \varnothing$ for $i = 1, \ldots, N$, $i \neq k$ (i.e., no coincidence of the eigenvalues of segment k with those of other segments). For this case, $S_{kn} = \{k\}$, and then Eq. 4.49 gives $B_{kn}(Y_k) = 0$ for all n. Further explanation can be found in Appendix 3.

For later reference, as with the A_{kn}'s, we may write the coefficients B_{jn} in Eqs. 4.48 and 4.49 in the form

$$B_{jn}(Y_k) = D_{jn}\phi_{jn}(Y_k), \tag{4.51}$$

where for $j \neq k$,

$$D_{jn}(Y) = \begin{cases} \dfrac{(-1)^{n+1}2(\gamma_k/L_k)}{L_j\left(\sum\limits_{i\in S_{jn}} (\gamma_i/L_i)\right)}, & \text{if } \beta_{jn} \in \Lambda_k; \\ 0, & \text{if } \beta_{jn} \notin \Lambda_k, \end{cases} \tag{4.52}$$

and when $j = k$,

$$D_{kn}(Y) = \frac{2}{L_k}\left(1 - \frac{(\gamma_k/L_k)}{\sum\limits_{i\in S_{kn}} (\gamma_i/L_i)}\right). \tag{4.53}$$

To illustrate the above cases, we consider the example in which $N = 3$, $L_1 = 1$, $L_2 = 2$, $L_3 = 2$, and $k = 2$ (the charge input is in segment 2). Then

$$\Lambda_1 = \{(2n + 1)\pi/2\}_{n=0}^{\infty}, \quad \Lambda_2 = \Lambda_3 = \{(2n + 1)\pi/4\}_{n=0}^{\infty}.$$

Hence, $\Lambda_2 \cap \Lambda_1 = \varnothing$, which is case *a* and thus

$$B_{1n} = 0 \quad \text{for } n = 0, 1, 2, \ldots.$$

Also, $\Lambda_2 \cap \Lambda_3 \neq \varnothing$, which is case *b*. The index sets defined in Eq. 4.50 are as follows,

$$S_{2n} = S_{3n} = \{2, 3\} \quad \text{for } n = 0, 1, 2, \ldots,$$

and by Eqs. 4.48 and 4.49 we have

$$B_{3n}(Y) = \frac{-\gamma_2}{(\gamma_2 + \gamma_3)}\cos(2n + 1)\frac{\pi}{4}(L_k - Y_k),$$

for $n = 0, 1, 2, \ldots,$

and

$$B_{2n}(Y) = \frac{\gamma_3}{(\gamma_2 + \gamma_3)}\cos(2n + 1)\frac{\pi}{4}(L_k - Y_k),$$

for $n = 0, 1, 2, \ldots.$

We note that this agrees with Eq. 4.37, which gives

$$B_{1n} = 0 \quad \text{and} \quad \gamma_2 B_{2n} + \gamma_3 B_{3n} = 0 \quad \text{for } n = 0, 1, 2, \ldots.$$

A GENERAL SOLUTION

The general problem Eqs. 3.9–3.13, denoted by (P), is linear and may be considered as composed of three subsidiary problems: the first being current injection in the branches only and no initial voltage distribution, the second being current injection at the soma only and no initial voltage distribution, and the third being no input currents, only an initial voltage distribution.

Current injection in the branches only

Using the Green's function G_j^k, the solution for an arbitrary current input I_k in the kth cylinder may be written as the convolution integral

$$V_j(X_j, T) = \int_0^{L_k}\int_0^T G_j^k(X_j, \xi_k, T - u)I_k(\xi_k, u)\,du\,d\xi_k \tag{5.1}$$

for $j = 1, \ldots, N$. The problem (P) is linear and thus the solution for arbitrary input currents $I_k(X_k, T)$, $k = 1, \ldots, N$ is

$$V_j(X_j, T) = \sum_{k=1}^{N}\int_0^{L_k}\int_0^T G_j^k(X_j, \xi_k, T - u)I_k(\xi_k, u)\,du\,d\xi_k \tag{5.2}$$

for $j = 1, \ldots, N$.

Current injection at the soma

The Green's function $G_j^s(X_j, T)$ for current injection at the soma is a solution of Eqs. 3.9–3.13 with

$$I_s = \delta(T), \quad I_j = 0, \quad F_j = 0, \quad j = 1, \ldots, N. \tag{5.3}$$

We define

$$G_j^s(0, T) = G_s^s(T) \tag{5.4}$$

when $X_j = 0$. The Laplace transform $\bar{G}_j^s$ is shown in Appendix 4 to be given by

$$\bar{G}_j^s = \frac{1}{(1 + \epsilon p + q\sigma)} \frac{\cosh q(L_j - X_j)}{\cosh qL_j}, \quad j = 1, \ldots, N, \quad (5.5)$$

Thus, we have

$$\bar{G}_j^s(X_j, p) = \frac{1}{\gamma_j} \bar{G}_j^j(0, X_j, p) = \frac{1}{\gamma_j} \bar{G}_s^j(X_j, p). \quad (5.6)$$

Hence, for an arbitrary input current I_s at the soma,

$$V_j(X_j, T) = \int_0^T G_j^s(X_j, T - u) I_s(u)\, du$$
$$= \frac{1}{\gamma_j} \int_0^T G_j^j(0, X_j, T - u) I_s(u)\, du \quad (5.7)$$

for $j = 1, \ldots, N$.

Initial voltage distribution

For the case of an initial voltage distribution, with no input currents $I_j, j = 1, \ldots, N$ or I_s, the problem may be restated as an equivalent problem in which we take

$$I_k(X_k, T) = F_k(X_k)\delta(T) \quad \text{and} \quad I_s(T) = F_s\delta(T) \quad (5.8)$$

for $k = 1, \ldots, N$ and $F_s = F_k(0)$ is the common value of the initial voltage distribution at the soma. The solution, by linearity, is given by

$$V_j(X_j, T) = \sum_{k=1}^{N} \int_0^{L_k} G_j^k(X_j, \xi_k, T) F_k(\xi_k)\, d\xi_k$$
$$+ \frac{1}{\gamma_j} G_j^j(0, X_j, T) F_s. \quad (5.9)$$

As the problem is linear, we can combine the results in Eqs. 5.2, 5.7, and 5.9 to give a general solution

$$V_j(X_j, T) = \sum_{k=1}^{N} \int_0^{L_k} \int_0^T G_j^k(X_j, \xi_k, T - u) I_k(\xi_k, u)\, du\, d\xi_k$$
$$+ \sum_{k=1}^{N} \int_0^{L_k} G_j^k(X_j, \xi_k, T) F_k(\xi_k)\, d\xi_k$$
$$+ \frac{1}{\gamma_j} G_j^j(0, X_j, T) F_s$$
$$+ \frac{1}{\gamma_j} \int_0^T G_j^j(0, X_j, T - u) I_s(u)\, du \quad (5.10)$$

where $j = 1, \ldots, N$ and F_s is the initial polarization at the soma.

ILLUSTRATIVE NUMERICAL EXAMPLES

We now illustrate the usefulness and certain features of the solutions obtained in the previous sections by considering the numerical examples below. In these examples, we use the dimensional forms of the solutions where from Eq. 3.6 we define the dimensional quantities

$$g_j^k = \frac{Q_0}{\gamma_k \tau_m} R_s G_j^k, \quad h_j^k = \frac{Q_0}{\gamma_k \tau_m} R_s H_j^k. \quad (6.1)$$

The large time solutions are numerically calculated by truncating the series after a suitable number of terms (see, for example, Poznanski, 1987*a, b;* Bluman and Tuckwell, 1987) with a simple bisection algorithm used to determine the roots α_n.

The effect of the "missing" roots β_{jn}

As a first example, we demonstrate the importance of including the solution K_j^k for the large time solution when electrotonic lengths are in odd integer ratios. However, this solution is not important because, as we shall show, small adjustments (say, for example, $\pm 10^{-6}$) to the electrotonic lengths of the involved cylinders satisfying the ratio criterion (Eq. 4.40) removes this solution with no discernable effect to the resulting waveform. Consequently, we may term the roots β_{jn} as missing from the transcendental Eq. 4.33 when the electrotonic lengths are in this ratio.

We consider a two-cylinder model ($N = 2$) with the following electrical values,

$$R_m = 4 \times 10^4\ \Omega\ \text{cm}^2, \quad C_m = 5 \times 10^{-7}\ F/\text{cm}^2,$$
$$R_i = 100\ \Omega\ \text{cm}, \quad d_s = 10^{-3}\ \text{cm},$$
$$R_{sh} = 1.27 \times 10^{10}\ \Omega, \quad l_1 = l_2 = 10^{-1}\ \text{cm}, \quad d_1 = d_2 = 10^{-4}\ \text{cm},$$

where these quantities are defined in Section 2. Hence, the following values may be calculated,

$$C_s = 1.57 \times 10^{-12}\ F, \quad R_s = 6.37 \times 10^9\ \Omega,$$
$$\tau_m = 20\ \text{ms}, \quad \tau_s = 10\ \text{ms}, \quad \lambda_1 = \lambda_2 = 10^{-1}\ \text{m},$$

where we have used

$$1/R_s = 1/R_{sh} + \pi d_s^2/R_m \quad (6.2)$$

The parameter values (Eq. 3.8) are

$$\gamma_1 = \gamma_2 = 5, \quad L_1 = L_2 = 1, \quad \epsilon = 0.5$$

In Table 1, we list the first 11 roots of the transcendental Eq. 4.33 and the roots β_{jn} given by Eq. 4.36. We note that consecutive roots of the β_{1n}'s lie between consecutive roots of the α_n's. For comparison, in Table 2, we

TABLE 1 The roots of the transcendental Eq. 4.33 in the case $L_1 = L_2 = 1$, and the roots $\beta_{1n} = \beta_{2n}$ (Eq. 4.36)

n	α_n	$\beta_{1n} = \beta_{2n}$
0	0.21658071	1.57079633
1	3.00857331	4.71238898
2	5.99941873	7.85398164
3	9.00628789	10.99557429
4	12.02798145	14.13716694
5	15.06452166	17.27875960
6	18.11508897	20.42035225
7	21.17825887	23.56194491
8	24.25237878	26.70353756
9	27.33582309	29.84513021
10	30.42712207	32.98672287

TABLE 2 **The roots of the transcendental Eq. 4.33 in the case $L_1 = 1.000001$ and $L_2 = 1$**

n	α_n	n	α_n
0	0.21658076	1	1.57079711
2	3.00857474	3	4.71239133
4	5.99942159	5	7.85398555
6	9.00629221	7	10.99557978
8	12.02798724	9	14.13717400
10	15.06452896	11	17.27876822
12	18.11509777	13	20.42036244
14	21.17826922	15	23.56195666
16	24.25239066	17	26.70355088
18	27.33583651	19	29.84514511
20	30.42713707	20	32.98673933

list the first 22 roots of the transcendental Eq. 4.33 for the "adjusted" case $L_1 = 1.000001$ and $L_2 = 1$. We remark that in this adjusted case, we now have the even numbered roots very close to the β_{1n}'s in Table 1. In this sense, as $L_1 \to L_2$, we "lose" these roots from the transcendental equation, and we may term the β_{1n}'s as missing.

Taking $Q_0 = 1pF$ and $Y_1 = 0.5$, the large time solutions g_j^1 (the full solution, see Eqs. 4.19 and 6.1) and h_j^1 (the full solution without the terms corresponding to the β_{jn}'s, see Eqs. 4.30 and 6.1) are plotted in Fig. 3 for the recording sites $X_1 = 0.8$ and $X_2 = 0.8$. At this point, we state that the waveforms h_1^1 and h_2^1 for the adjusted case $L_1 = 1.000001$ and $L_2 = 1$ overlap g_1^1 and g_2^1 plotted in Fig. 3 for the "unadjusted" case. We note that the solutions h_1^1 and h_2^1 in the unadjusted case coincide. This is apparent from the expression 4.34, which is symmetric with respect to recording site when electrotonic lengths of the recording cylinders are the same, i.e., for $j \neq i$, $H_j^k(X_j, Y_k, T) = H_i^k(X_i, Y_k, T)$ when $L_j = L_i$ and $X_j = X_i$. More generally, if we consider the case $L_1 = L_2 = \cdots = L_N$, then the solution to Eqs. 4.24–4.27 is $K_j^k \equiv 0$ and the solution H_j^k to Eqs. 4.20–4.23 is symmetric with respect to X_j. We may define $G(X, Y, T) = H_j^k(X_j, Y_k, T)$ for $j = 1, \ldots, N$, where $X = X_j$ and $Y = Y_k$, and then G satisfies the problem

$$\text{in } 0 < X < L, \quad T > 0 \qquad \frac{\partial^2 G}{\partial X^2} - \frac{\partial G}{\partial T} - G = 0; \tag{6.3}$$

$$\text{at } X = L \qquad \frac{\partial G}{\partial X} = 0; \tag{6.4}$$

$$\text{at } X = 0 \qquad G = G_s, \tag{6.5}$$

and

$$G_s + \epsilon \frac{dG_s}{dT} - \gamma \frac{\partial G}{\partial X} = 0; \tag{6.6}$$

$$\text{at } T = 0, \quad 0 \le X \le L \quad G = \delta(X - Y); \tag{6.7}$$

where $\gamma = \sum_{j=1}^{N} \gamma_j$.

Thus, G is the Green's function to the single cylinder problem given by Eqs. 6.3–6.7 (compare with Poznanski, 1987*b* and Bluman and Tuckwell, 1987 for the case $\epsilon = 1$). Hence, in this degenerate case, when all the cylinders are equal, the solution H_j^k represents the solution to the equivalent single cylinder problem in Eqs. 6.3–6.7. Thus, intuitively, omitting the terms corresponding to the roots β_{jn} is equivalent to collapsing the cylinders together when electrotonic lengths are equal.

The small and large time solutions

For the previous example, we show in Fig. 4 the small time solution in Eq. 4.13, in the case $X_2 = 0.8$. We show the effect of retaining more terms ($n = 4$, 5, 6, and 8) of the series for the large time solution of g_2^1. As n increases, the large time solution g_2^1 becomes accurate for smaller times, but there comes a point at which retaining more terms becomes unfeasible, and then the small time solution should be used to obtain the response for earlier times. An overlap region between the small and large time solutions can always be found by retaining a sufficient number of terms in the large time expression. In this way, the two expressions can be used to obtain the solution for all time. In the example plotted in Fig. 4, we see the high degree of accuracy obtained with the large time solution when only eight terms of the series are retained. We also mention that a simulation with a compartmental model for this example gives a waveform that passes through the early and late time (with $n = 8$)

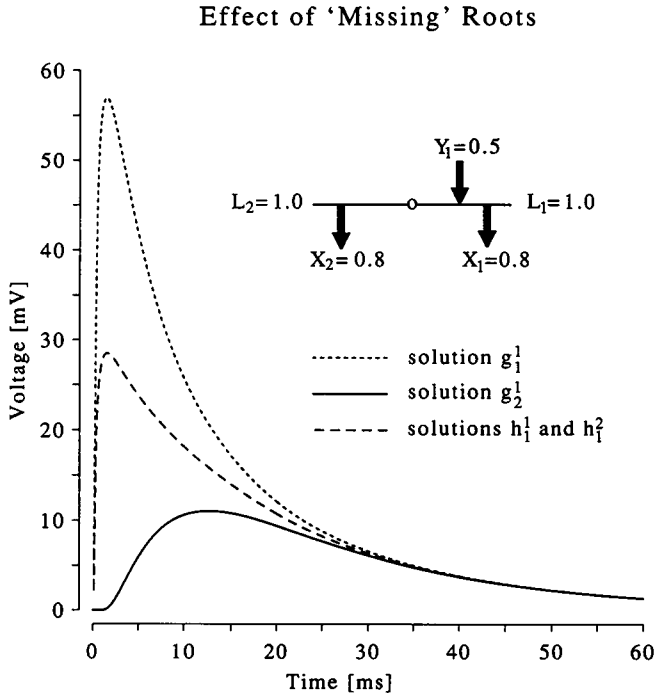

FIGURE 3 Voltage response for a two-cylinder model ($\epsilon = 0.5$) with symmetric recording sites $X_1 = 0.8$ in cylinder 1 ($L_1 = 1$) and $X_2 = 0.8$ in cylinder 2 ($L_2 = 1$) and a charge input site at $Y_1 = 0.5$ in cylinder 1. The large time solutions are shown at both recording sites X_1 and X_2 for the full solution g_j^1 and the partial solution h_j^1, where $j = 1, 2$, respectively, for X_1 and X_2.

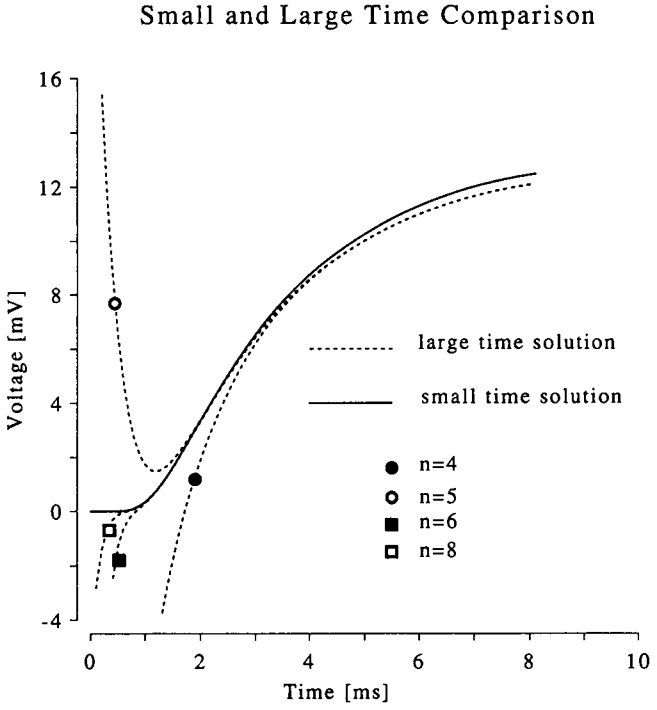

FIGURE 4 A comparison of the small and large time solutions for the two-cylinder model shown in Fig. 3, with the recording site at $X_2 = 0.8$ and the same input site. The large time solution is shown for the cases when $n = 4$, 5, 6, and 8 terms of the series are retained.

solutions (for which they are valid) and their overlap region.

The effect of the shunt at the soma

To show the effect of an increasing amount of shunt at the soma, we consider a two-cylinder model with the electrical values of R_m, C_m, R_i, d_s, d_1, and d_2 taken to be the same as those in the previous examples with $l_1 = 0.1$ cm, $l_2 = 0.2$ cm, and R_{sh} variable. Thus, we have C_s, τ_m, λ_1, and λ_2, as given in Section 6.1, with the parameter values

$$\gamma_1 = \gamma_2 = 5, \quad L_1 = 1, \quad L_2 = 2.$$

We consider the values (correct to 3 sf) (*a*) $R_{sh} = \infty\ \Omega$, (*b*) $R_{sh} = 1.27 \times 10^{10}\ \Omega$, (*c*) $R_{sh} = 1.41 \times 10^{9}\ \Omega$, and (*d*) $R_{sh} = 6.70 \times 10^{8}\ \Omega$, which give

(*a*) $R_s = 1.27 \times 10^{13}\ \Omega$, $\tau_s = 20$ ms and $\epsilon = 1$

(*b*) $R_s = 6.37 \times 10^{12}\ \Omega$, $\tau_s = 10$ ms and $\epsilon = 0.5$

(*c*) $R_s = 1.27 \times 10^{12}\ \Omega$, $\tau_s = 2$ ms and $\epsilon = 0.1$

(*d*) $R_s = 6.37 \times 10^{11}\ \Omega$, $\tau_s = 1$ ms and $\epsilon = 0.05$

Taking $Q_0 = 1\,pF$ and $Y_1 = 0.75$, the large time solution of g_2^1 (retaining 20 terms of the series) is plotted in Fig. 5 for the recording site $X_2 = 1$ and for each of the above values of R_{sh}. It can be seen that an increasing shunt reduces the peak voltage and speeds the final decay. Also, it is worth remarking that the shunt has little effect on the early parts of the transients. This is predicted by the early time solution in Eq. 4.13, the leading order terms of which are independent of R_{sh}, because we can write

$$\gamma_j/\epsilon = g_{\infty j}/g_{sm} \quad \text{and} \quad h = \sum_{j=1}^{N} g_{\infty j}/g_{sm}.$$

Thus, the leading order terms of both Eqs. 4.13 and 4.17 are independent of R_{sh}, as is the scaling used in Eq. 6.1, which can be shown to be

$$g_j^k = \frac{Q_0}{\tau_m g_{\infty k}} G_j^k$$

The effect of adding cylinders

In this example, we consider a three-cylinder model, with R_m, C_m, R_i, d_s, and R_{sh} as given in the preceding examples. We take

$$l_1 = 0.1 \text{ cm}, \quad l_2 = 0.2 \text{ cm}, \quad l_3 = 0.15 \text{ cm},$$
$$d_1 = d_2 = d_3 = 10^{-4} \text{ cm}.$$

These give C_s, R_s, τ_m, and τ_s, as before, and $\lambda_1 = \lambda_2 = \lambda_3 = 0.1$ cm. The parameter values in Eq. 3.8 are

$$\gamma_1 = \gamma_2 = \gamma_3 = 5, \quad L_1 = 1, \quad L_2 = 2, \quad L_3 = 1.5, \quad \epsilon = 0.5$$

Taking $Q_0 = 1\,pF$ and $Y_1 = 0.8$, the large time solution of g_1^1 is plotted in Fig. 6 for the recording site $X_1 = 0.2$ and for the cases $N = 1$, 2, 3, respectively. Thus, with the

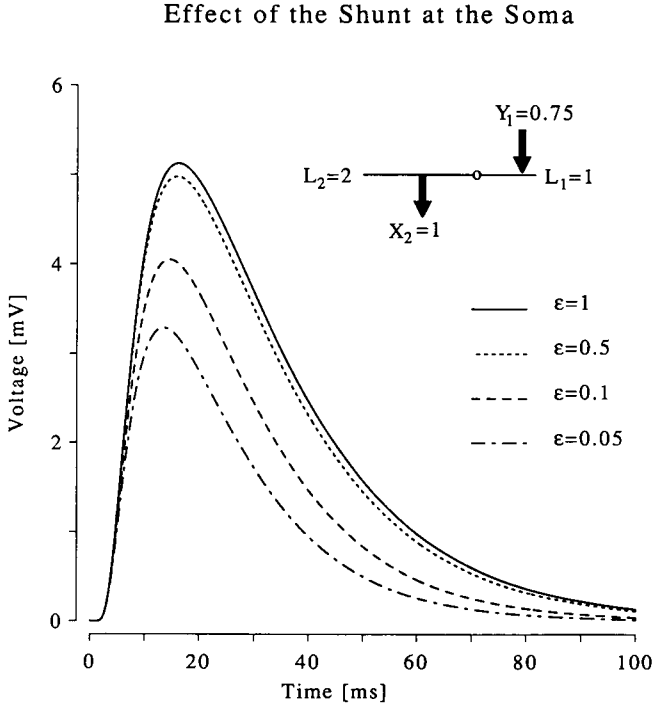

FIGURE 5 Illustration of the effect of an increasing shunt resistance at the soma for a two-cylinder model ($L_1 = 1$, $L_2 = 2$) with input site at $Y_1 = 1$ in cylinder 1 and recording site at $X_2 = 1$ in cylinder 2. The large time solution g_2^1 is shown for the cases $\epsilon = 1$, 0.5, 0.1, and 0.05.

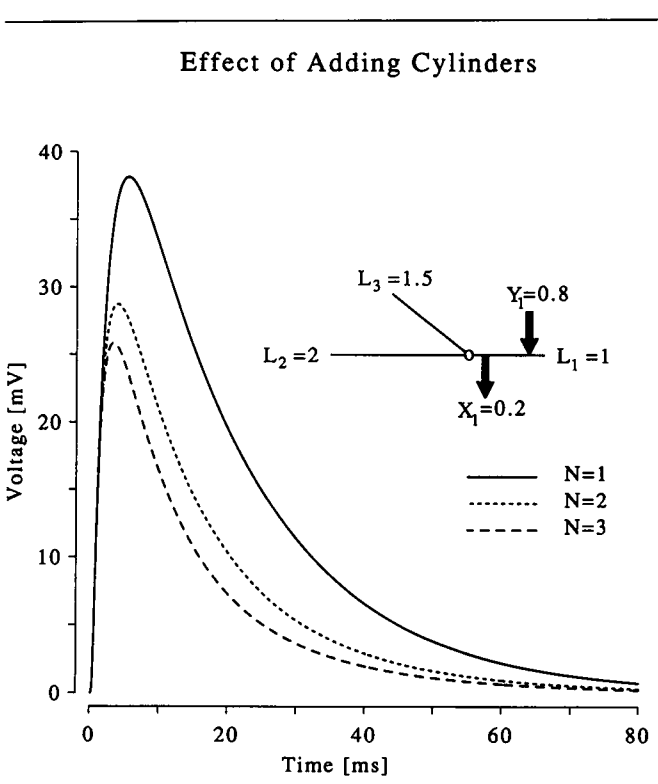

FIGURE 6 Voltage response for the recording site $X_1 = 0.2$ and input site $Y_1 = 0.5$ in cylinder 1 with $L_1 = 1$ and $\epsilon = 0.5$, in the cases of (*a*) no added cylinders ($N = 1$), (*b*) one added cylinder ($N = 2$) with $L_2 = 2$, and (*c*) two added cylinders ($N = 3$) with $L_2 = 2$ and $L_3 = 1.5$.

same input and recording conditions, this example shows the effect on the resulting waveform: first by adding a cylinder of electrotonic length $L_2 = 2$ and second by adding a cylinder of electrotonic length $L_3 = 1.5$ to the original cylinder of electrotonic length $L_1 = 1$. We note that again the early times are hardly affected, but the late times deviate as the charge spreads into the other cylinders.

SUMMARY AND CONCLUSIONS

(*a*) We present a set of equations that are used to define a passive cable model of a neurone with a soma and shunt and one or more dendritic trees represented by equivalent cylinders, which can have different electrotonic lengths.

(*b*) The model equations are analyzed for the case of a point charge input in one of the cylinders. An eigenfunction expansion (separation of variables technique) is used to derive the voltage response (Eq. 4.19) in the form of a series of exponentially decaying components in Eqs. 4.30 and 4.34. The expression for G_j^k can be written in the convenient form

$$G_j^k(X_j, Y_k, T) = \sum_{n=0}^{\infty} E_{kn}\psi_{kn}(Y_k)\psi_{jn}(X_j)e^{-(1+\alpha_n^2)T} + \sum_{n=0}^{\infty} D_{jn}\phi_{kn}(Y_k)\phi_{jn}(X_j)e^{-(1+\beta_{jn}^2)T}, \quad (7.1)$$

using Eqs. 4.44 and 4.51. We find it convenient to consider the problem for G_j^k as the sum of two subproblems (see Eq. 4.19) and then to use separation of variables to each of these problems. The reasons for this are twofold:

(1) First, ease of computation of the eigenvalues, eigenfunctions, and amplitudes. By considering G_j^k in the form Eq. 4.19, we find we divide the set of eigenvalues into one set that is common to the whole system, the α_n's (see Eq. 4.33), and a second set specifically related to a particular branch, the β_{jn}'s (see Eq. 4.36). These are relatively easy to compute, because the α_n's are given by the roots of a transcendental Eq. 4.33 and the β_{jn}'s are given explicitly in Eq. 4.36. Consequently, standard techniques then yield the eigenfunctions and corresponding amplitudes, which may be obtained explicitly. When separation of variables is applied directly to G_j^k, we find that the corresponding eigenvalues are given by the roots of the following transcendental equation,

$$\prod_{i=1}^{N} \cos(\alpha L_i)[1 - \epsilon(1 + \alpha^2)] = \alpha \sum_{j=1}^{N} \gamma_j \sin \alpha L_j \prod_{\substack{i=1 \\ i\neq j}}^{N} \cos(\alpha L_i). \quad (7.2)$$

Analysis of this equation leads naturally to the two sets of eigenvalues. The α_n's arise when $\prod_{i=1}^{N} \cos(\alpha L_i) \neq 0$, and dividing through by this quantity in Eq. 7.2 gives Eq. 4.33. Alternatively, if $\prod_{i=1}^{N} \cos(\alpha L_i) = 0$, then we obtain the β_{jn}'s. Thus, in this respect, we are led to the consideration of the two problems H_j^k and K_j^k in Eq. 4.32.

(2) Second, the K_j^k problem in practical computations of the solution is unimportant. We qualify this by noting that the K_j^k problem has the trivial solution unless the ratio of the lengths of equivalent cylinders are in odd integer ratios (see Eq. 4.40). Thus, whenever these cases arise, small adjustments to the lengths of the involved cylinders remove the K_j^k from the solution, with no significant effects on the overall waveforms (Section 6.1).

We may write Eq. 7.1 in the dimensional form as follows,

$$g_j^k(x_j, y_k, t) = \sum_{n=0}^{\infty} e_n\psi_{kn}(y_k/\lambda_k)\psi_{jn}(x_j/\lambda_j)e^{-t/\tau_n} + \sum_{n=0}^{\infty} d_{jn}\phi_{kn}(y_k/\lambda_k)\phi_{jn}(x_j/\lambda_j)e^{-t/\tau_{jn}}, \quad (7.3)$$

on using Eq. 3.7, where

$$g_j^k = \frac{Q_0}{\gamma_k\tau_m} R_s G_j^k, \; e_n = \frac{Q_0}{\gamma_k\tau_m} R_s E_{kn}, \; d_{jn} = \frac{Q_0}{\gamma_k\tau_m} R_s D_{jn}, \quad (7.4)$$

$$y_k = \lambda_k Y_k, \; \tau_n = \frac{\tau_m}{(1 + \alpha_n^2)}, \; \tau_{jn} = \frac{\tau_m}{(1 + \beta_{jn}^2)}, \quad (7.5)$$

where y_k is the physical distance of the input site from the soma. We remark on some important features of the solution:

(i) The time constants may be categorized into two sets: the first are the τ_n's, which are common to the whole system and independent of stimulation Y_k and recording position X_j, and the second are the τ_{jn}'s, which are associated with a particular branch and dependent on the recording segment j.

(ii) The amplitudes of the two series are affected by stimulation and recording positions. The set of amplitudes for the first series in Eq. 7.3 has three parts: the first is e_n, a constant depending only on the model parameters and the corresponding time constant, the second depending on the input (or excitation) site, and the third varying with the recording position.

(iii) We note the symmetry of the response solution with regard to input and recording sites; interchanging them does not affect the resulting waveform form for a particular stimulus.

(*c*) The expression Eq. 7.1, although valid for all T, is only practically useful in numerical calculations for obtaining the large time behavior. For smaller times, more terms in the series have to be retained to obtain a required accuracy. An alternative expansion valid for small time is obtained in Section 4.2 by expanding the solution Eqs. 4.10 and 4.11 of the Laplace transform problem for G_j^k, see Eqs. 4.4–4.8, for large values of the transform parameter, and inverting to obtain Eqs. 4.13 and 4.17. These two alternative expansions for G_j^k may be used to calculate the voltage response efficiently for all values of T.

(*d*) For completeness, we include the relevant convolution integrals for the voltage response to arbitrary input currents (Section 5).

(*e*) These results may be extended to include the fully branched structure, i.e., several dendritic trees emanating from a common soma. At branch points, we have current conservation and voltage continuity and thus have a particular case of the Eqs. 3.9–3.13, with appropriate modification of the boundary condition Eq. 3.10. A recursive definition of the system may then be set up, with daughter segments at one level becoming parent segments for the next level, moving outward along dendritic trees from soma to tips to give the required branched structure.

(*f*) Finally, in the particular case of only one equivalent cylinder, the results derived in Sections 4 and 5 reduce to those obtained by Poznanski (1987*b*) and, when $\epsilon = 1$, to those by Bluman and Tuckwell (1987).

APPENDIX 1

To solve Eqs. 4.4–4.8, we proceed as follows:

(*a*) The solution of Eq. 4.5, which satisfies Eq. 4.6, may be written as

$$\bar{G}_j^k(X_j, Y_k, p) = A \frac{\cosh q(L_j - X_j)}{\cosh qL_j}, \qquad \text{(A1.1)}$$

where $j \neq k$, q is defined in Eq. 4.11, and A is a constant that is independent of the recording segment because of the continuity condition in Eq. 4.7.

(*b*) To solve Eq. 4.4, we note that in the kth segment, the domain $(0, L_k)$ must be divided into two distinct regions, namely $0 < X_k < Y_k$ and $Y_k < X_k < L_k$, because of the presence of the delta function at $X_k = Y_k$. Hence, for $X_k > Y_k$, the solution of Eq. 4.4 that satisfies Eq. 4.6 may be written as

$$\bar{G}_k^k(X_k, Y_k, p) = C \frac{\cosh q(L_k - X_k)}{\cosh qL_k}, \qquad \text{(A1.2)}$$

with C a constant to be determined, and for $X_k < Y_k$, the solution of Eq. 4.4 may be written in the form

$$\bar{G}_k^k(X_k, Y_k, p) = A \frac{\cosh q(L_k - X_k)}{\cosh qL_k} + B \sinh qX_k, \qquad \text{(A1.3)}$$

where A and B are constants. This satisfies the continuity condition at the soma Eq. 4.7, comparing with Eq. A1.1.

(*c*) Using Eqs. A1.1 and A1.3 in Eq. 4.8, we obtain

$$A(1 + \epsilon p) = -Aq \sum_{j=1}^{n} \gamma_j \tanh qL_j + \gamma_k qB, \qquad \text{(A1.4)}$$

which on rearranging gives

$$A = \frac{\gamma_k q}{(1 + \epsilon p + q\sigma)} B, \qquad \text{(A1.5)}$$

where σ is given in Eq. 4.11.

(*d*) We are now left with two constants A and B to be determined by satisfying the conditions across the source at $X_k = Y_k$. These conditions are implicitly contained in Eq. 4.4 (see, for example, Stakgold, 1979, chapter 1) and may be written as

$$\lim_{X_k \to Y_k+} \bar{G}_k^k(X_k, Y_k, p) = \lim_{X_k \to Y_k-} \bar{G}_k^k(X_k, Y_k, p), \qquad \text{(A1.6)}$$

and

$$\lim_{X_k \to Y_k+} \frac{\partial \bar{G}_k^k(X_k, Y_k, p)}{\partial X_k} - \lim_{X_k \to Y_k-} \frac{\partial \bar{G}_k^k(X_k, Y_k, p)}{\partial X_k} = -1. \qquad \text{(A1.7)}$$

The condition Eq. A1.6 simply states that G_k^k is continuous at $X_k = Y_k$, and Eq. A1.7 states that the jump in the X_k derivative of $\bar{G}_k^k$ at $X_k = Y_k$ is of magnitude -1.

Using Eqs. A1.2 and A1.3 with Eqs. A1.5 in A1.6 gives

$$B\left\{\frac{\gamma_k q}{(1 + \epsilon p + q\sigma)} \frac{\cosh q(L_k - Y_k)}{\cosh qL_k} + \sinh qX_k\right\} = C \frac{\cosh q(L_k - Y_k)}{\cosh qL_k}. \qquad \text{(A1.8)}$$

Similarly, using Eqs. A.11 and A.12 in Eq. A1.7 gives

$$(C - A)q \frac{\sinh q(L_k - Y_k)}{\cosh qL_k} + Bq \cosh qY_k = 1. \qquad \text{(A1.9)}$$

Using Eq. A1.5 in Eq. A1.9, we may solve Eqs. A1.8 and A1.9 for B to obtain on simplification

$$B = \frac{1}{q} \frac{\cosh q(L_k - Y_k)}{\cosh qL_k}. \qquad \text{(A1.10)}$$

Thus, Eq. A1.8 gives

$$C = \frac{\gamma_k}{(1 + \epsilon p + q\sigma)} \frac{\cosh q(L_k - Y_k)}{\cosh qL_k} + \frac{1}{q} \sinh qY_k, \quad \text{(A1.11)}$$

and Eq. A1.5 gives

$$A = \frac{\gamma_k}{(1 + \epsilon p + q\sigma)} \frac{\cosh q(L_k - Y_k)}{\cosh qL_k}. \quad \text{(A1.12)}$$

Hence, we obtain Eqs. 4.9 and 4.10.

APPENDIX 2

The coefficients A_{kn} and B_{jn} in the expansions in Eqs. 4.30 and 4.34 are now derived using certain orthogonality conditions satisfied by the eigenfunctions in Eqs. 4.32 and 4.35. The initial conditions in Eqs. 4.28 and 4.29 give, on using Eqs. 4.30 and 4.34,

$$\delta(X_k - Y_k) = \sum_{n=0}^{\infty} A_{kn}(Y_k)\psi_{kn}(X_k) + \sum_{r=0}^{\infty} B_{kr}(Y_k)\phi_{kr}(X_k); \quad \text{(A2.1)}$$

$$0 = \sum_{n=0}^{\infty} A_{kn}(Y_k)\psi_{jn}(X_j) + \sum_{r=0}^{\infty} B_{jr}(Y_k)\phi_{jr}(X_j), \quad j \neq k. \quad \text{(A2.2)}$$

We now discuss the orthogonality conditions satisfied by the two sets of eigenfunctions in Eqs. 4.32 and 4.34.

A modified orthogonality condition for the ψ_{jn}'s

Because the ψ_{kn} are not orthogonal over $0 \le X_k \le L_k$, a modified orthogonality condition (similar to that used by Churchill, 1942) is used to derive the A_{kn}'s. If we use Eq. 4.18 in Eqs. 3.9–3.13 and use the eigenfunction expansion of Eqs. 4.30 and 4.34, we obtain for the ψ_{kn}'s,

$$\text{in } 0 < X_k < L_k \quad \psi''_{kn} + \alpha_n^2\psi_{kn} = 0; \quad \text{(A2.3)}$$

$$\text{at } X_k = L_k \quad \psi'_{kn} = 0; \quad \text{(A2.4)}$$

$$\text{at } X_k = X_j = 0 \quad \psi_{kn} = \psi_{jn}, \quad \text{(A2.5)}$$

and

$$(1 - \epsilon(1 + \alpha_n^2))\psi_{kn} - \sum_{j=1}^{N} \gamma_j\psi'_{jn} = 0; \quad \text{(A2.6)}$$

for $j = 1, \ldots, N$, where $'$ denotes differentiation with respect to X_j in the jth segment.

Proceeding formally, we consider Eqs. A2.3–A2.6 for ψ_{kn} and ψ_{km} to obtain (see, for example, Titchmarsh, 1962, p. 1),

$$\int_0^{L_k} \psi_{kn}\psi_{km}\, dX_k = \frac{1}{(\alpha_m^2 - \alpha_n^2)}[\psi'_{kn}(0)\psi_{km}(0) - \psi_{kn}(0)\psi'_{km}(0)]. \quad \text{(A2.7)}$$

To eliminate the unknown derivatives from Eq. A2.7, we consider the boundary condition at $X_k = 0$ for ψ_{kn} and ψ_{km},

$$\epsilon(\alpha_m^2 - \alpha_n^2)\psi_{kn}(0)\psi_{km}(0) + \sum_{j=1}^{N} \gamma_j[\psi_{jn}(0)\psi'_{jm}(0) - \psi_{jm}(0)\psi'_{jn}(0)] = 0, \quad \text{(A2.8)}$$

where we have used the continuity of ψ_{jn} at $X_j = 0$. If we substitute Eq. A2.7 with k set to j into Eq. A2.8, we may solve immediately for the desired orthogonality condition

$$\mathcal{B}(\Psi_n, \Psi_m) \equiv \sum_{j=1}^{N} \gamma_j \int_0^{L_j} \psi_{jn}\psi_{jm}\, dX_j + \epsilon\psi_{kn}(0)\psi_{km}(0) = 0, \quad \text{(A2.9)}$$

where $n \neq m$, and defining $\Psi_n(X)$ by

$$\Psi_n(X) = \psi_{jn}(X_j), \quad \text{for } X = X_j. \quad \text{(A2.10)}$$

Integrating when $n = m$, we thus have the result

$$\mathcal{B}(\Psi_n, \Psi_m) = \begin{cases} \tfrac{1}{2}\sum_{j=1}^{N} \gamma_j L_j \sec^2 \alpha_n L_j + \tfrac{1}{2}\theta_n + \epsilon, & \text{if } n = m; \\ 0, & \text{if } n \neq m, \end{cases} \quad \text{(A2.11)}$$

where θ_n is given after Eq. 4.42, except in the case $\epsilon = 1$ and $n = m = 0$ when

$$\mathcal{B}(\Psi_0, \Psi_0) = 1 + \sum_{j=1}^{N} \gamma_j L_j. \quad \text{(A2.12)}$$

Thus, for any function F that can be expressed as

$$F_j(X_j) = \sum_{n=0}^{\infty} A_{kn}\psi_{jn}, \quad \text{for } j = 1, \ldots, N, \quad \text{(A2.13)}$$

where F_j is the component of F in jth branch, we have that

$$A_{kn} = \frac{\mathcal{B}(F, \Psi_n)}{\mathcal{B}(\Psi_n, \Psi_n)}, \quad \text{(A2.14)}$$

where the definition of $\mathcal{B}(\cdot, \cdot)$ in Eq. A.29 is extended for arbitrary functions.

An orthogonality condition for the ϕ_{jn}'s

The eigenfunctions ϕ_{jn} are orthogonal over the interval $0 \le X_j \le L_j$, and using standard notation, we have

$$\langle \phi_{jn}, \phi_{jm} \rangle \equiv \int_0^{L_j} \phi_{jn}(X_j)\phi_{jm}(X_j)\, dX_j = \begin{cases} L_j/2, & \text{if } n = m; \\ 0, & \text{if } n \neq m. \end{cases} \quad \text{(A2.15)}$$

The coefficients A_{kn} and B_{jn}

Using Eq. A2.15 in Eqs. A2.1 and A2.2 gives,

$$B_{kr}(Y_k) = \left(\frac{2}{L_k}\right)\phi_{kr}(Y_k) - \left(\frac{2}{L_k}\right)\sum_{n=0}^{\infty} A_{kn}(Y_k)\langle \psi_{kn}, \phi_{kr} \rangle; \quad \text{(A2.16)}$$

$$B_{jr}(Y_k) = -\left(\frac{2}{L_j}\right)\sum_{n=0}^{\infty} A_{kn}(Y_k)\langle \psi_{jn}, \phi_{jr} \rangle \quad j \neq k; \quad \text{(A2.17)}$$

where it can be shown that

$$\langle \psi_{jn}, \phi_{jr} \rangle = \frac{(-1)^r\beta_{jr}}{(\beta_{jr}^2 - \alpha_n^2)} \quad \text{(A2.18)}$$

for $j = 1, \ldots, N$, because $\alpha_n \neq \beta_{jr}$. To obtain the A_{kn}, we rearrange Eqs. A2.1 and A2.2 to give

$$\delta(X_k - Y_k) - \sum_{r=0}^{\infty} B_{kr}(Y_k)\phi_{kr}(X_k) = \sum_{n=0}^{\infty} A_{kn}(Y_k)\psi_{kn}(X_k); \quad \text{(A2.19)}$$

$$-\sum_{r=0}^{\infty} B_{jr}(Y_k)\phi_{jr}(X_j) = \sum_{n=0}^{\infty} A_{kn}(Y_k)\psi_{jn}(X_j), \quad j \neq k; \quad \text{(A2.20)}$$

which is in the form of Eq. A2.13, with F defined as

$$F_k(X_k) = \delta(X_k - Y_k) - \sum_{r=0}^{\infty} B_{kr}(Y_k)\phi_{kr}(X_k); \quad \text{(A2.21)}$$

$$F_j(X_j) = -\sum_{r=0}^{\infty} B_{jr}(Y_k)\phi_{jr}(X_j), \quad j \neq k. \quad \text{(A2.22)}$$

Thus, proceeding formally,

$$\begin{aligned}\mathcal{B}(F, \Psi_n) &= \sum_{j=1}^{N} \gamma_j \int_0^{L_j} F_j\psi_{jn}\, dX_j + \epsilon F_j(0)\psi_{kn}(0) \\ &= \gamma_k\psi_{kn}(Y_k) \\ &\quad - \sum_{j=1}^{N} \gamma_j \int_0^{L_j} \sum_{r=0}^{\infty} \{B_{jr}(Y_k)\phi_{jr}(X_j)\psi_{jn}(X_j)\}\, dX_j \\ &= \gamma_k\psi_{kn}(Y_k) \\ &\quad - \sum_{j=1}^{N} \sum_{r=0}^{\infty} \{\gamma_j B_{jr}(Y_k)\langle\psi_{jn}, \phi_{jr}\rangle\}, \quad \text{(A2.23)}\end{aligned}$$

where integration and summation may be interchanged, because the series in the second line of Eq. A2.22 converges uniformly on $(0, L_j)$. The double series in the last expression in Eq. A2.23 can be shown to be zero, on using Eqs. A2.18 and 4.37. Thus, in convenient notation, we obtain

$$A_{kn} = \frac{\mathcal{B}(\Delta, \Psi_n)}{\mathcal{B}(\Psi_n, \Psi_n)}, \quad \text{(A2.24)}$$

where

$$\Delta(X) = \begin{cases} \delta(X_k - Y_k), & \text{if } X = X_k; \\ 0, & \text{otherwise,} \end{cases} \quad \text{(A2.25)}$$

that when evaluated agrees with the A_{kn} of Eqs. 4.42 and 4.43 derived from the Laplace transform solution. Note that nothing has been proven about the completeness of the ψ_{jn}'s and the ϕ_{jn}'s for representing an arbitrary function.

APPENDIX 3

In this appendix, we explain how the residues of $\bar{G}_j^k$ are evaluated to obtain the coefficients A_{kn} given in Section 4.3.1.1 and the B_{jn} given in Section 4.3.1.2.

First, we analyze the expression for $\bar{G}_j^k$ given in Eq. 4.41. The first series in Eq. 4.41 has simple poles at $p = -(1 + \alpha_n^2)$ or equivalently $q = i\alpha_n$ using Eq. 4.11, and the second series has simple poles at $p = -(1 + \beta_{jn}^2)$ or $q = i\beta_{jn}$. It is easily verified that no α_n coincides with any β_{jn}, i.e., the sets Λ_j (see Eq. 4.38) are each disjoint with the set $\{\alpha_n\}_{n=0}^{\infty}$. Thus, the simple poles of the two series are independent of the segment considered, unlike those of the second series that are segment dependent.

Residues at p = $-(1 + \alpha_n^2)$

If $p = -(1 + \alpha_n^2)$, then we write $\bar{G}_j^k$ in the form

$$\bar{G}_j^k = \frac{h(p)}{k(p)}, \quad \text{(A3.1)}$$

where we define

$$k(p) = 1 + \epsilon(q^2 - 1) + q\sigma, \quad \text{(A3.2)}$$

noting that q and σ are functions of p (see Eq. 4.11), and $h(p)$ we define as the rest of the expression in Eq. 4.9. It is easily shown that at $p = -(1 + \alpha_n^2)$

$$k(p) = 0, \quad k'(p) \neq 0 \quad \text{and} \quad h(p) \neq 0, \quad \text{(A3.3)}$$

where $'$ denotes differentiation with respect to p. Evaluating Eqs. 4.41 and 4.9 at $X_j = 0$, we have (see, for example, Priestley, 1985, chapter 7)

$$A_{kn} = \frac{h(p)}{k'(p)}, \quad \text{at } p = -(1 + \alpha_n^2), \quad \text{(A3.4)}$$

which gives Eq. 4.42 on using the relations $\cosh iz = \cos z$, $\sinh iz = i \sin iz$ for z complex. However, we must distinguish the particular case $\epsilon = 1$ and $n = 0$ because $\alpha_n = 0$. The residue $p = -1$ may still be evaluated using Eq. A3.3 but cannot be deduced by setting $\epsilon = 1$ and $n = 0$ in the expression in Eq. 4.42.

Residues at p = $-(1 + \beta_n^2)$

Precisely the same approach as that outlined above may be adopted to evaluate the residues at $p = -(1 + \beta_{jn}^2)$. In this case, we note that Eqs. 4.9 and 4.10 have simple poles at $p = -(1 + \beta_{jn}^2)$ if both $\cosh qL_k = 0$ and $\cosh qL_j = 0$ for some $j \neq k$ (there may be more than one such j, which is accounted for by the sets S_{jn} given in Eq. 4.50). We find it convenient to analyze Eqs. 4.9 and 4.10 for simple poles and residues by considering the two cases as stated above in the determination of the Bjn's. These simply distinguish between the case when eigenvalues of a recording branch do not coincide with those in the stimulating branch (case (a)), and the alternative case when some (or all) the eigenvalues of the recording branch do coincide with some (or all) of those in the stimulating segment (case (b)).

APPENDIX 4

The problem for $\bar{G}_s^k$, as for $\bar{G}_j^k$ (see Eqs. 4.3–4.8), can be shown to be,

$$\text{in } 0 < X_j < L_j \quad \frac{\partial^2 \bar{G}_j^s}{\partial X_j^2} - (1 + p)\bar{G}_j^s = 0; \quad \text{(A4.1)}$$

$$\text{at } X_j = L_j \quad \frac{\partial \bar{G}_j^s}{\partial X_j} = 0; \quad \text{(A4.2)}$$

$$\text{at } X_j = 0 \quad \bar{G}_j^k = \bar{G}_s^s, \quad \text{(A4.3)}$$

and

$$(1 + \epsilon p)\bar{G}_s^s - \sum_{j=1}^{N} \gamma_j \frac{\partial \bar{G}_j^s}{\partial X_j} = 1; \quad \text{(A4.4)}$$

for $j = 1, \ldots, N$. The solution to Eq. A4.1 that satisfies Eq. A4.2 and continuity at the soma Eq. A4.3 is

$$\bar{G}_j^s = A \frac{\cosh q(L_j - X_j)}{\cosh qL_j} \quad \text{(A4.5)}$$

for $j = 1, \ldots, N$ where A is a constant, determined by Eq. A4.5 satisfying Eq. A4.4. Immediately we obtain Eq. 5.5 on using the expressions in Eq. 4.11.

We thank Dr. A. B. Tayler and Dr. J. J. B. Jack for many helpful comments.

Financial support from the Science and Engineering Research Council, the U.S. Army (grant N00614-86-J-1027), and the Wellcome Trust is gratefully acknowledged.

Received for publication 24 October 1991 and in final form 1 April 1992.

REFERENCES

Abramowitz, M., and I. Stegun, editors. 1965. Handbook of Mathematical Functions. Dover, New York. 1046 pp.

Bluman, G., and H. Tuckwell. 1987. Techniques for obtaining solution for Rall's model neuron. *J. Neurosci. Methods.* 20:151–166.

Carslaw, H. S., and J. C. Jaeger. 1959. Conduction of Heat in Solids. 2nd ed. Oxford University Press, Oxford. 510 pp.

Churchill, R. V. 1942. Expansions in series of non-orthogonal functions. *Bull. Am. Math. Soc.* 48:143–149.

Durand, D. 1984. The somatic shunt cable model for neurons. *Biophys. J.* 46:645–653.

Holmes, W. R., and W. Rall. 1987. Estimating the electrotonic structure of neurons which cannot be approximated as equivalent cylinders. *Soc. Neurosci. Abstr.* 13:1517.

Jack, J. J. B., D. Noble, and R. W. Tsien. 1975. Electric current flow in excitable cells. Oxford University Press, Oxford. 518 pp.

Kawato, M. 1984. Cable properties of a neuron model with non-uniform membrane resistivity. *J. Theor. Biol.* 111:149–169.

Poznanski, R. R. 1987*a*. Transient responses in a somatic shunt cable model for synaptic input activated at the terminal. *J. Theor. Biol.* 127:31–50.

Poznanski, R. R. 1987*b*. Techniques for obtaining analytical solutions for the somatic shunt cable model. *Math. Biosci.* 83:1–23.

Priestley, H. A. 1985. Introduction to Complex Analysis. Oxford University Press, Oxford. 197 pp.

Rall, W. 1959. Branching dendritic trees and motoneurone membrane resistivity. *Exp. Neurol.* 1:491–527.

Rall, W. 1960. Membrane potential transients and membrane time constant of motoneurons. *Exp. Neurol.* 2:503–532.

Rall, W. 1962. Theory of physiological properties of dendrites. *Ann. NY Acad. Sci.* 96:1071–1092.

Rall, W. 1969. Time constants and electronic length of membrane cylinders and neurons. *Biophys. J.* 9:1483–1508.

Rall, W. 1977. Core conductor theory and cable properties of neurons. *In* Handbook of Physiology. Section 1. The Nervous System. Volume 1. E. R. Kandel, editor. *Am. Physiol. Soc.*, Bethesda, MD. 37–97.

Segev, I., and W. Rall. 1983. Theoretical analysis of neuron models with dendrites of unequal lengths. *Soc. Neurosci. Abstr.* 9:341.

Spiegal, M. R. 1965. Laplace Transforms. McGraw-Hill, New York. 285 pp.

Stakgold, I. 1979. Green's Functions and Boundary Value Problems. Wiley-Interscience, New York. 638 pp.

Titchmarsh, E. C. 1962. Eigenfunction Expansions—Part I. 2nd ed. Oxford University Press, Oxford. Oxford. 203 pp.

Tuckwell, H. C. 1987. Introduction to Mathematical Neurobiology. Vol. 1. Linear Cable Theory and Dendritic Structure. Cambridge University Press, Cambridge. 291 pp.

Van Dyke, M. 1964. Perturbation Methods in Fluid Mechanics. Academic Press, New York. 229 pp.

Walsh, J. B., and H. C. Tuckwell. 1985. Determination of the electrical potential over dendritic trees by mapping onto a nerve cylinder. *J. Theor. Neurobiol.* 4:27–46.